Nitromethane Decomposition under High Static Pressure

Margherita Citroni,*,† Roberto Bini,†,‡ Marco Pagliai,‡ Gianni Cardini,†,‡ and Vincenzo Schettino†,‡

European Laboratory for Nonlinear Spectroscopy (LENS), via Nello Carrara 1, 50019 Sesto Fiorentino, Italia, and Dipartimento di Chimica, Università di Firenze, via della Lastruccia 3, 50019 Sesto Fiorentino, Italia

Received: April 20, 2010; Revised Manuscript Received: June 8, 2010

The room-temperature pressure-induced reaction of nitromethane has been studied by means of infrared spectroscopy in conjunction with ab initio molecular dynamics simulations. The evolution of the IR spectrum during the reaction has been monitored at 32.2 and 35.5 GPa performing the measurements in a diamond anvil cell. The simulations allowed the characterization of the onset of the high-pressure reaction, showing that its mechanism has a complex bimolecular character and involves the formation of the aci-ion of nitromethane. The growth of a three-dimensional disordered polymer has been evidenced both in the experiments and in the simulations. On decompression of the sample, after the reaction, a continuous evolution of the product is observed with a decomposition into smaller molecules. This behavior has been confirmed by the simulations and represents an important novelty in the scene of the known high-pressure reactions of molecular systems. The major reaction product on decompression is *N*-methylformamide, the smallest molecule containing the peptide bond. The high-pressure reaction of crystalline nitromethane under irradiation at 458 nm was also experimentally studied. The reaction threshold pressure is significantly lowered by the electronic excitation through two-photon absorption, and methanol, not detected in the purely pressure-induced reaction, is formed. The presence of ammonium carbonate is also observed.

Introduction

Nitromethane, a liquid-insensitive high explosive, is the prototype of the nitro-organic compounds, a family of molecules containing the NO_2 group bonded to an organic moiety through a C−N bond. These are energetic molecules that, when subjected to heat or shock waves, undergo a fast and highly exothermic chemical reaction leading to the formation of gaseous compounds.[1] The molecular mechanism of detonation is not well understood to date, though its knowledge and control would be of interest in the design of novel insensitive and high energetic materials, which is now mostly performed on a phenomenological basis. In particular, understanding the mechanism of the detonation initiation, i.e., how many molecules and which chemical bonds are involved in the first steps of the reaction, would be of great importance in the production of safe and efficient explosives or propellants. In this respect, understanding the mechanism of the high-pressure and high-temperature reactivity of nitromethane would be of primary importance in view of the simplicity of its molecular structure.

In the gas phase, thermal decomposition of nitromethane involves as the first step the intramolecular homolytic cleavage of the C−N bond,[2,3] whereas in condensed phases experimental data[4−6] and theoretical predictions[7,8] suggest that the temperature- or pressure-induced chemical reactions involve two or more molecules in the initial step, even if they ultimately result in a decomposition into small gaseous molecules. In particular, time-resolved Raman measurements under stepwise loading[5,6] revealed an intensification of intermolecular interactions involving the H atoms, evidenced by a broadening of the C−H symmetric stretching mode and by a softening of the C−N stretching mode in the first steps of the reaction. The role of intermolecular interactions involving the migration of an H atom or an H^+ ion is supported by the evidence that nitromethane is sensitized by small quantities of amines both in static compression experiments[9] and under shock waves.[10] Sensitization likely occurs through the formation of the aci-ion of nitromethane (Figure 1), consequent to the abstraction of an H atom by the basic amine molecule.[11] Engelke et al.[12] provided experimental evidence that the aci-ion is also present in pure liquid ni-

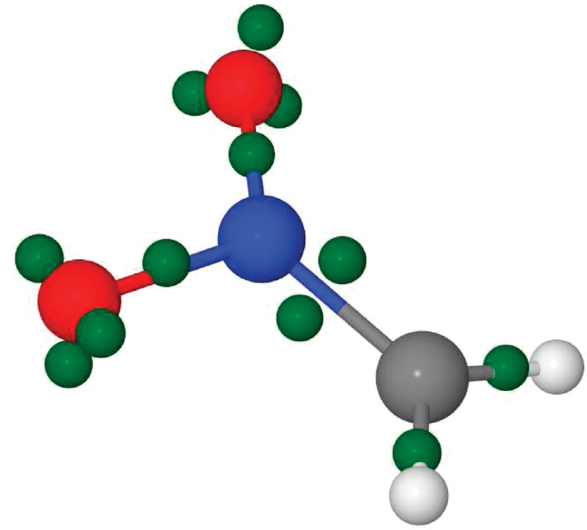

Figure 1. Electronic structure of the aci-ion $CH_2NO_2^-$ as extracted from the molecular dynamics simulation discussed in the text. The Maximally Localized Wannier Centers (MLWC) are reported in green. The H atoms are indicated in white, the C atoms in gray, the N atoms in blue, and the O atoms in red.

* To whom correspondence should be addressed. E-mail: margherita@lens.unifi.it.
† LENS.
‡ Dipartimento di Chimica.

10.1021/jp1035508
Published on Web 07/07/2010

tromethane at high pressure (2 GPa and 81 °C), in a concentration 1000 times larger than that at room conditions. It was also demonstrated that irradiation with UV light increases the room pressure concentration of the aci-ion.[13] Car−Parrinello molecular dynamics simulation of the reactivity of hot (3000−4000 K) and dense ($V/V_0 = 0.68-0.61$) liquid nitromethane[8] showed that in these extreme conditions the first step of the reaction is an intermolecular proton abstraction leading to the formation of $CH_3NO_2H^+$ and the aci-ion $CH_2NO_2^-$, with a concerted mechanism involving at least three nitromethane molecules.

The decomposition reaction of nitromethane under high static pressure has been studied in the liquid[4] and solid phase[9,14,15] from room temperature to 350 °C. There is consensus on the strong increase of the reaction rate with increasing temperature or pressure, the latter observation indicating a negative activation volume and thus suggesting a bimolecular reaction mechanism. However, the reaction product, composed of a solid and a fluid phase, has not been characterized. The lack of a Raman signal suggested that the product of the reaction is a solid amorphous compound.[14] On the basis of the infrared[4,9] and mass spectra,[4] the solid product of the high-pressure thermal decomposition (at temperatures above 100 °C and pressures from 2 to 7 GPa) has been suggested to be primarily ammonium oxalate[9] or a mixture of ammonium formate and water.[4] On the other side, the high-pressure (28−50 GPa) room-temperature reaction product has been reported[15] to be a dark yellow liquid amorphous polymer containing a variety of functional groups as suggested by the infrared spectrum.

In the present work, the pressure-induced reaction of nitromethane at room temperature has been studied in full detail with a combined experimental and theoretical approach. The time evolution of the reaction has been monitored by infrared spectroscopy obtaining definite evidence of a bimolecular reaction mechanism. This is fully supported by the results of ab initio molecular dynamics simulations in the Car−Parrinello approach based on a recently proposed crystal structure determination of nitromethane up to the high-pressure reaction threshold of 32 GPa.[16] The connection of the reaction mechanism with the details of the crystal structure is evidenced in a solid state reactivity point of view. Particular attention has been devoted to the characterization of the reaction product evidencing some unique features of the nitromethane reaction. At high pressure, an extended three-dimensional disordered compound is obtained as attested by both experimental and computational results. The disordered compound cannot be quenched at room pressure. On decreasing the pressure, the polymeric array decomposes giving rise to a number of small volatile molecules. The nonvolatile product of the reaction can be identified as mainly composed by *N*-methylformamide. The experimental behavior monitored by infrared spectroscopy is nicely reproduced in the molecular dynamics simulation, and the resulting molecules can be at least partly identified. The effect of laser irradiation on the high-pressure reaction of nitromethane has also been studied showing that, as reported for other molecular crystals, two-photon absorption significantly lowers the high-pressure reaction threshold. The spectrum is similar to that of the pure pressure-induced reaction with important additional features. On decreasing the pressure, besides formamide the presence of methanol and ammonium carbonate can be identified.

Experimental Methods

A membrane diamond anvil cell (DAC), equipped with IIa-type diamonds, was used to generate high pressure. Rhenium gaskets were used for all of the experiments. A fresh sample of liquid nitromethane, ≥99% from Aldrich, was loaded for each experiment. The initial sample diameter was 100 μm. In most experiments, the sample was either loaded in a gasket about 35 μm thick or deposited as a 10 μm thick layer on a KBr pellet previously formed in the DAC.

The IR spectra were recorded with a Bruker IFS-120HR FTIR spectrometer, modified to allow measurements in the DAC,[17] in the mid-IR region 600−5000 cm^{-1} with a spectral resolution of 1 cm^{-1}. The pressure was determined by the ruby fluorescence technique, using as the excitation source the 2nd harmonic of a cw Nd:Yag laser (532 nm) with a power lower than 0.5 mW to avoid unintended photochemical effects. The photochemical behavior of nitromethane at high pressure was probed by irradiation with 100 mW of the 458 nm Ar^+ laser line, focused in such a way to irradiate the sample uniformly.

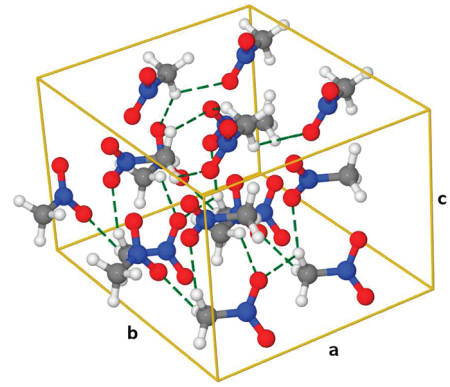

Figure 2. Image of the crystal structure of nitromethane at 15 GPa resulting from the simulation. The solid lines indicate the edges of the simulation cell, as described in the text. The H atoms are indicated in white, the C atoms in gray, the N atoms in blue, and the O atoms in red. The dotted lines indicate the shortest intermolecular O···H distances (≤2.3 Å).

Computational Details

A series of ab initio molecular dynamics simulations of the nitromethane reaction under high pressure have been performed with the Car−Parrinello method (CPMD).[18,19] All the calculations have been carried out using the BLYP[20,21] exchange-correlation functional along with a 80 Ry cutoff of the plane waves expansion of the Kohn−Sham orbitals. Norm conserving Martins−Troullier[22] pseudopotentials with Kleinman−Bylander[23] decomposition have been adopted for all atoms, and the equations of motion have been integrated with a time step of 1 au (0.02419 fs) for a time ranging from 40 000 to 180 000 steps at each volume except for the last simulation at 750 K, where the time step has been increased gradually until 4 au (0.0968 fs) after the system did not show any further reactivity.

Preliminary calculations on a sample with 16 molecules (i.e., with two unit cells in the *a* and *b* directions) confirmed the results reported by Citroni et al.[16] showing that, despite the poor representation of the van der Waals interactions, the present approach reasonably reproduces the crystal structure and the vibrational spectra of nitromethane at pressures below the reaction threshold. The minor relevance of the correction for the van der Waals interactions, in this case, has been discussed by Conroy et al.[24] For the purpose of the present work, a major point is that the adopted approach nicely reproduces the network of hydrogen bonds (Figure 2) that is a key feature of the crystal structure at high pressure[16] and for the onset of the high-pressure chemical reaction, as will be discussed in the following.

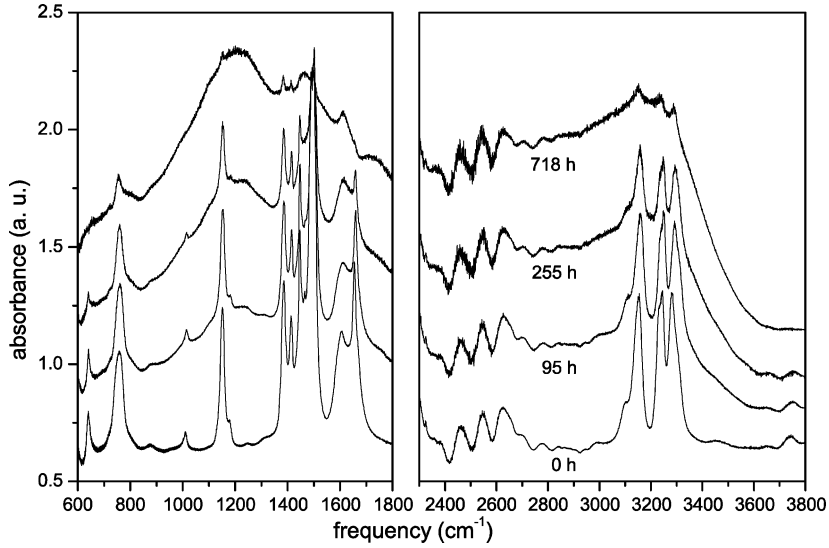

Figure 3. FTIR spectra of a ~10 μm thick sample of nitromethane, deposited on a KBr pellet, at 32 GPa as a function of time. The absorbances are calculated using a reference spectrum made on a KBr pellet in the DAC.

Simulations of the chemical reaction of nitromethane were carried out on a sample of 16 molecules in a simulation box of 2 unit cells in the *a* and *b* directions and 1 unit cell in the *c* direction. The initial unit cell parameters were chosen as the experimental values at 1.1 GPa. The pressure was gradually increased stepwise to give starting configurations for constant-volume simulations at different densities. The final products were kept for about 180 000 steps (~4 ps) at 300 K without observing any further reaction. The reverse procedure was followed to enlarge the simulation box to reach a final density comparable to that experimentally observed at ambient pressure and 300 K. At this temperature, the reaction evolution on decreasing the pressure is very slow, and to increase the reaction rate the temperature was gradually raised by velocity scaling to 750 K, continuing the simulation until no further reaction was observed for about 50 ps, on a simulation of more than 100 ps.

To understand the changes of the electronic structure and the initial steps of the reaction pathway, selected configurations have been characterized by calculating the Maximally Localized Wannier functions.[25−27] These are obtained by minimizing the spread of the Wannier functions (w_n) in the real space

$$S = \sum_{n=1}^{N} (\langle w_n|r^2|w_n\rangle - \langle w_n|\mathbf{r}|w_n\rangle^2) \qquad (1)$$

Maximally Localized Wannier functions have also been used to identify and characterize the species obtained during the decompression. To correctly select the chemical species present in the sample, the final configurations have been inspected applying periodic boundary conditions.

Results and Discussion

High-Pressure Reaction. In all of the experiments, the pressure was increased in steps of 1−2 GPa, and the FTIR spectrum was measured at each step after pressure stabilization. The evolution of the absorption frequencies, intensities, and bandwidths on compression reproduces exactly the behavior previously found and reported in ref 16. To precisely locate the reaction threshold pressure, the FTIR spectrum of a thin layer (~10 μm) of nitromethane deposited on a KBr pellet was monitored for more than 24 h at all the pressure steps above 21 GPa, to detect any spectral change ascribable to a chemical transformation. At 32.3 GPa, after an induction time of about 3 h, the first spectral modifications due to a chemical reaction were observed. The pressure was maintained between 32.3 and 32.1 GPa for the whole duration of the reaction. The FTIR spectrum was monitored until no more changes occurred with time, which was after about 680 h (see Figure 3). Another thin CH_3NO_2 sample (~5 μm) deposited on a KBr pellet was pressurized, in steps of 1−3 GPa, up to 35.5 GPa. At this pressure, the transformation was completed in 120 h. Different experiments on pure nitromethane samples were carried out to check if the presence of the KBr pellet affected the reaction pressure threshold and evolution or the recovered products. No significant differences could be observed.

The reaction is characterized by the slow growth of very strong and broad absorptions in the regions 900−1700 and 2500−3500 cm^{-1}, with maxima at about 1200 and 3200 cm^{-1}, and by a corresponding decrease of intensity of the nitromethane absorptions (Figure 3). When the spontaneous evolution of the spectrum is completed, a small amount of nitromethane is still present. The broad and almost structureless spectrum is clear evidence that the reaction product is an amorphous extended polymeric array. The assignment of the observed spectral features is not straightforward considering also, in the regions of lower intensity absorptions, the overlap with the interference fringes between the diamond faces delimiting the sample. However, it can be said with confidence that the structureless absorption centered at ~3200 cm^{-1} arises from strongly associated −OH, −NH, or −NOH groups. In this region, features to be assigned to saturated −CH bonds can also be recognized. The broad band centered at ~1200 cm^{-1} likely arises from vibrations of CO, CC, CN, and NO single bonds. It is remarkable that the overall shape of the band is reminiscent of the broad feature observed in the same region for the high-pressure decomposition product of furane and assigned to CC and CO single bonds.[28] In the present case, the band is considerably broader, as expected. Weak features in the spectrum observed at ~1735 and ~1600 cm^{-1} can likely be associated with CO or NO double bonds, as is also suggested by the further reaction evolution on decreasing the pressure, as will be discussed in the next section.

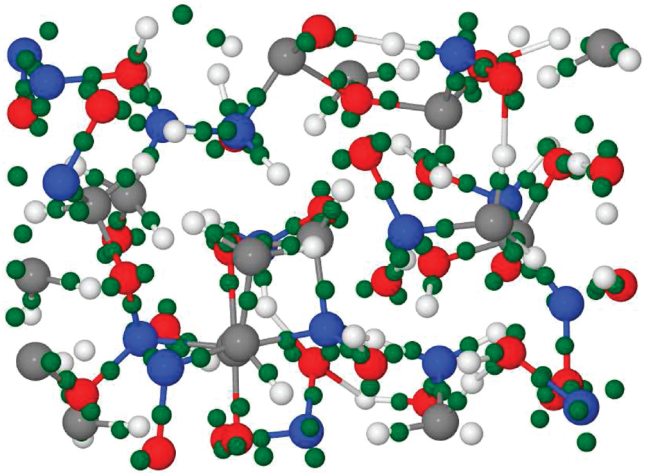

Figure 4. Simulation cell at the end of the compression. The H atoms are indicated in white, the C atoms in gray, the N atoms in blue, the O atoms in red, and the MLWC in green.

The results of the molecular dynamics simulation are of considerable help to figure out the possible structure of the high-pressure reaction product. In the simulation, a reaction is observed at $V/V_0 < 0.43$, much smaller than experimental ($V/V_0 < 0.67$). This is due to the need of accelerating the reaction in the simulation and to the already mentioned poor representation of the van der Waals interactions.[29] Figure 4 shows the structure of the simulation cell at the end of the reaction. It can be seen that a complex three-dimensional array of chemical bonds is formed with terminal −COH, −CNH, −NOH, −CNOH, and −CH bonds that nicely account for the high-frequency part of the experimental spectrum. In the inside of the array, we find CNO, CON, NCO, OCO, and ONO sequences that all give rise to absorption frequencies in the region around 1200 cm^{-1}. As a whole, the molecular dynamics simulation indicates that the complex absorption spectrum does not result from the overlap of spectra of different reaction products but from a single amorphous three-dimensional array.

Reaction on Decreasing the Pressure. The high-pressure reaction product described in the previous section is metastable and cannot be quenched at ambient pressure. In fact, on decreasing the pressure, the infrared spectrum changes substantially as can be seen from Figure 5. In particular, the prominent broad feature at ∼1200 cm^{-1} decreases in intensity and disappears at pressures below 15 GPa. At the same time, a strong band at ∼1700 cm^{-1} develops below 20 GPa to finally become the strongest band in the spectrum. Only minor changes, on the contrary, are observed on decompression in the region around ∼3200 cm^{-1}, apart from the complete disappearance of the residual nitromethane peaks. This indicates the persistence of strongly associated hydrogen bonded groups. When the pressure in the membrane is completely released (with a residual pressure on the sample of 1.8 GPa), the sample appeared transparent in transmission on observation with the microscope with inclusion of some gas bubbles. Actually, a peculiar feature of the spectrum of the decompressed sample is the appearance of a sharp peak at 2350 cm^{-1} clearly assigned to carbon dioxide. The formation of carbon dioxide has also been reported in the thermal decomposition (20−50 GPa, 100−160 °C) of nitromethane.[9] Opening the cell in a N_2 atmosphere causes in most cases a complete loss of the product. However, occasionally on cell opening a part of the sample was left in the cell, probably adsorbed on the KBr pellet, and the resulting infrared spectrum is reported in Figure 6.

These experimental observations are, at least qualitatively, nicely reproduced in the molecular dynamics simulation. In fact, on decreasing the pressure, the high-pressure three-dimensional array decomposes and at room pressure gives a number of small molecules (including water, CO_2, formaldehyde, formic acid, dihydroxylamine, a NH_3OH^- complex) together with larger molecules. These latter seem to be unstable, and in fact, they further decompose on heating at 500 and 700 K. A list of the molecules observed in the simulation on decompression is shown in Figures 1 and 2 of the Supporting Information.

The spectrum of the reaction product after decreasing the pressure and the cell opening (Figure 6) closely resembles, but is not exactly equal to, the spectrum of the product reported by Pruzan et al.[15] from experiments carried out at room pressure and 50 GPa. Comparison of the spectrum of the recovered sample after decompression and cell opening with the spectrum of a sample of *N*-methylformamide compressed to 4.7 GPa and decompressed (Figure 6) allows us with some confidence to identify this residual reaction product as *N*-methylformamide. In fact, the position and relative intensity of the most intense bands, the amide I (1670 cm^{-1}), amide II (1540 cm^{-1}), and the band at 1390 cm^{-1}, to be likely assigned as the C−H bending mode, match very nicely, apart from the significant broadening of the bands of the product as a consequence of the residual stress. This is remarkable considering that the amide bands are generally sensitive to the environment.[30,31] Unfortunately, the weakness of the spectrum in the lower frequency region and the overlap with the interference fringes prevents us from gathering further evidence for this identification. However, the comparison of the spectrum in the 3200 cm^{-1} region is in good agreement with identification of the product as *N*-methylformamide. This result is of considerable interest since the product contains the prototype peptide bond. The basic binding unit of biochemistry is thus formed in a high-pressure reaction from an apparently unrelated molecule.

The molecular dynamics simulation cannot account for the details of the formation of this reaction product since the conditions (temperature and pressure) of the simulation differ from experiments. However, it is rewarding that both formic acid and ammonia are observed on decompression. It can also be noted that the formation of *N*-hydroxyformamide is observed in the molecular dynamics simulation. It is quite possible that the peptide bond is produced by condensation of some of the small molecules formed from the decomposition of the high-pressure polymeric array.

Reaction Mechanism. The time evolution of the intensity of the nitromethane IR absorption bands during the reaction has been used for a kinetic analysis. The absorption band due to the ν_{12} mode of nitromethane, at 32.3 and 35.5 GPa, was fitted to a pseudo-Voigt profile, and the integrated intensity $y(t)$, proportional to the nitromethane concentration, is reported as a function of time in Figure 7. The band was chosen because it is isolated, always in scale and with a sufficient intensity. The time evolution of $y(t)$ was fitted to the Avrami equation,[32] a rate law describing a process of nucleation, i.e., formation of reactive sites and diffusion-controlled nuclei growth inside a material.

$$y(t) = y_0 - (y_0 - y_\infty)[1 - \exp[-k(t + t_0)^n]] \qquad (2)$$

In eq 2, y_0 is the integrated area at time t_0; y_∞ is the integrated intensity when the reaction evolution is completed; t_0 represents the induction time; n is a parameter related to the spatial distribution of the nuclei growth; and k is the rate constant.[32] The results of the fit are reported in Table 1. The value $n = 2$

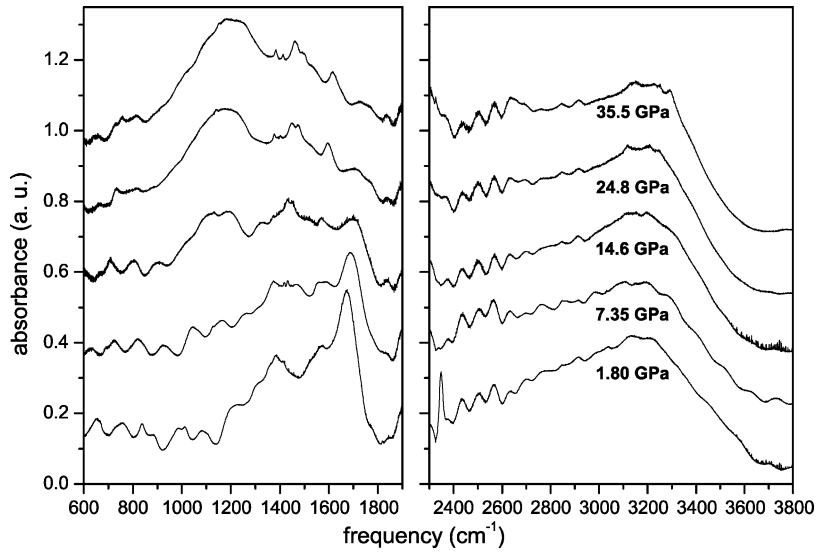

Figure 5. FTIR spectra of a ~5 μm thick sample of nitromethane, deposited on a KBr pellet, on decompression after the spontaneous reaction at 35.5 GPa. The absorbances are calculated using a reference spectrum made on a KBr pellet in the DAC.

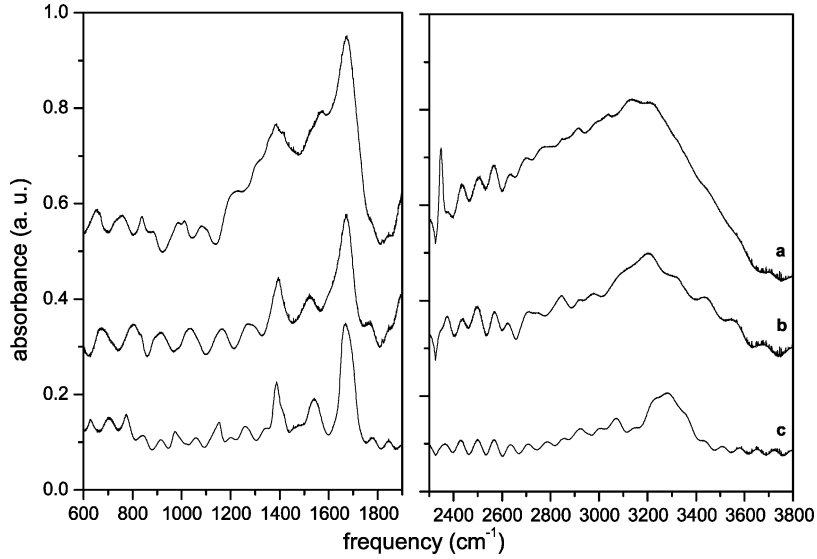

Figure 6. Trace **a**: FTIR spectrum of the reaction product before the cell opening after decompression, with a residual pressure of 1.80 GPa (~5 μm thick sample deposited on a KBr pellet). Trace **b**: FTIR spectrum of the reaction product at room pressure after cell opening (~5 μm thick sample deposited on a KBr pellet). Trace **c**: FTIR spectrum of *N*-methylformamide in the DAC at room pressure after compression to 4.70 GPa (~5 μm thick sample deposited on a KBr pellet). The absorbances are calculated using a reference spectrum made on a KBr pellet in the DAC.

implies a three-dimensional nuclei growth with a nucleation rate decreasing with time. The positive value of t_0 indicates an induction time for the reaction. Our data show that the induction time is much smaller at 35.5 than at 32.2 GPa. Even though we have only two data points, the marked increase of the reaction rate with pressure can be taken as a further proof that the activation volume of the reaction is negative, and thus the reaction proceeds through at least a bimolecular mechanism. This is supported by the results of the molecular dynamics simulation.

The first stage of the reaction mechanism has been investigated by the Maximally Localized Wannier Centers (MLWC)[25−27] and can be described in four steps (see Figure 8):

• A nitromethane molecule deformed by the neighboring molecules (panel **a**) loses a proton and forms the $CH_2NO_2^-$ ion (panel **b**) with a double bond localized between the carbon and the nitrogen atom.

• The H^+ ion is attracted by an oxygen of a neighboring nitromethane molecule and forms a CH_3NOOH^+ ion (panel **b**). The positive charge is localized on the nitrogen atom.

• The bond between the H^+ and the deformed nitro group is not very stable, and the H^+ ion moves close to the nitro group of another molecule (panel **c**). A positive charge is present on the nitrogen and a negative charge on one of the O atoms of the nitro group of the nitromethane that has lost the H^+ ion.

• The two charges are very close to each other, and a covalent N−O bond forms; the H^+ is attracted back by the oxygen atom forming an OH group (panel **d**).

This reaction mechanism onset is quite reasonable if the crystal structure is taken into account. In fact, the crystal structure of nitromethane is stabilized above 11 GPa by the presence of N−O···H hydrogen bonds extending along the three crystallographic directions (especially *a* and *b*).[16] At 15 GPa, the minimum O···H distance is 2.16 Å, but several inequivalent

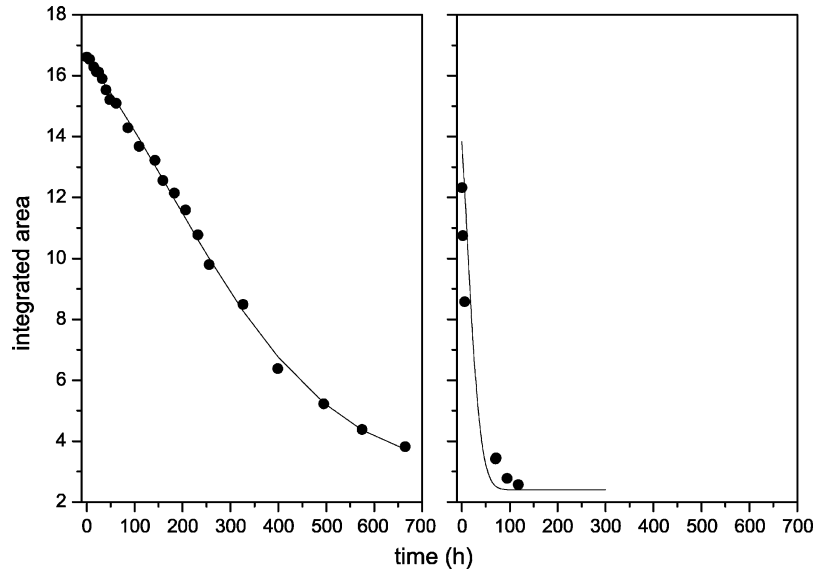

Figure 7. Time decay of the integrated area of the mode ν_{12} of nitromethane during the reaction at 32.2 GPa (left panel) and at 35.5 GPa (right panel). Circles: experimental data. Lines: fit to the Avrami equation.

TABLE 1: Kinetic Parameters Obtained from the Fit to the Avrami Equation

reaction P (GPa)	y_0	y_∞	n	k (h^{-1})	t_0 (h)	χ^2
32.2	18.4	3.0	2.0	3.5×10^{-6}	179	0.04
35.5	16.0	2.4	1.9	9.2×10^{-4}	15	0.04

O···H distances have very similar values, with ∠OHC angles ranging from 122° to 140°, creating an extended network of intermolecular H-bonds. The lack of phase transitions up to the reaction pressure, and the volume contraction (V/V_0 is 0.65 at 15 GPa and 0.60 at 27 GPa[16]) that involves the three crystallographic axes in a comparable amount, make it very reasonable that the first step of the reaction involves an H^+ migration and that later the reaction is propagated along nearly any direction in the crystal. Consistently, the reaction kinetics for the formation of this extended compound can be described by an Avrami equation, deriving from a model of growth of a new phase inside a material, where a fast nucleation is followed by a diffusion-controlled nuclei growth in the three directions.

Photoassisted Pressure-Induced Reaction. The UV absorption spectrum of nitromethane[33,34] consists of a strong absorption centered at 198 nm (extending from 165 to 225 nm) assigned to a $\pi \rightarrow \pi^*$ transition and a much weaker absorption centered at 270 nm (extending from 250 to 355 nm) mainly due to a $\sigma \rightarrow \pi^*$ transition, overlapped to a forbidden $n \rightarrow \pi^*$ transition. The involved molecular orbitals are all localized on the nitro group (including the σ orbital of the C−N bond),[33] and, assuming a C_{2v} symmetry, the three transitions mentioned correspond to excitations from the fundamental $\tilde{X}\ ^1A_1$ state to $^1B_1$, $^1B_2$, and $^1A_2$ states, respectively. The band gap in the nitromethane crystal has been calculated to be 3.28 eV (378 nm)[35] or 3.61 eV (344 nm)[36] at room pressure and to decrease by about 0.4[35,37] or 0.23 eV,[36] depending on the calculation method, in the pressure range 0−20 GPa. A significant lowering of the reaction threshold pressure by excitation to the first electronic states has been reported in several crystalline molecular systems[38] and is due to the attainment of highly reactive structures after decay to the ground electronic state.[39,40]

A 35 μm thick sample of pure nitromethane was used to probe the effects of laser irradiation on the high-pressure reactivity. After loading, the pressure was raised in steps of 2 GPa, waiting for pressure stabilization and monitoring the FTIR spectrum at each step. Irradiation cycles of 3−4 h with 100 mW of 514 or 458 nm laser light were performed at 12 GPa, and no changes were observed in the FTIR spectrum before and after irradiation. At 15.0 GPa, irradiation with 100 mW at 458 nm induced an extremely slow chemical transformation. The 458 nm line is absorbed through a two-photon process, presumably matching the $\pi \rightarrow \pi^*$ transition. Hence, we performed irradiation cycles at 18.5 GPa until the transformation reached a stationary state.

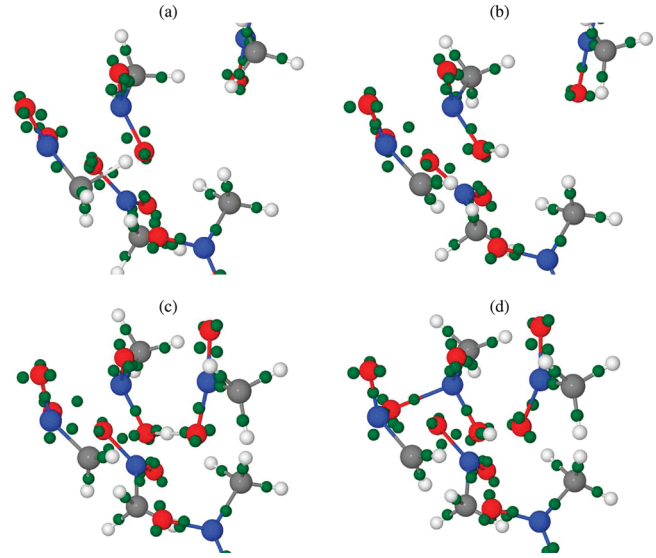

Figure 8. Mechanism of the reaction onset as obtained by the simulation. The H atoms are indicated in white, the C atoms in gray, the N atoms in blue, the O atoms in red, and the MLWC in green. (**a**) The C−H bond starts to break. (**b**) The H^+ ion migrates to the O atom of the neighbor molecule. The $CH_2NO_2^-$ and CH_3NOOH^+ ions are formed. (**c**) A third molecule attracts the H^+, while the N atom of the CH_3NOOH^+ ion and an O atom of the aci-ion start forming a new N−O bond. (**d**) The new N−O bond is formed, and the formed species contains a terminal OH group.

The evolution of the infrared spectrum during the irradiation (Figure 9) is qualitatively similar to that observed in the purely pressure-induced reaction. The nitromethane peaks at 710 and 1120 cm^{-1} do not disappear completely. Other nitromethane peaks are only barely visible probably because they are heavily overlapped with the product bands. Also, in this case the reaction

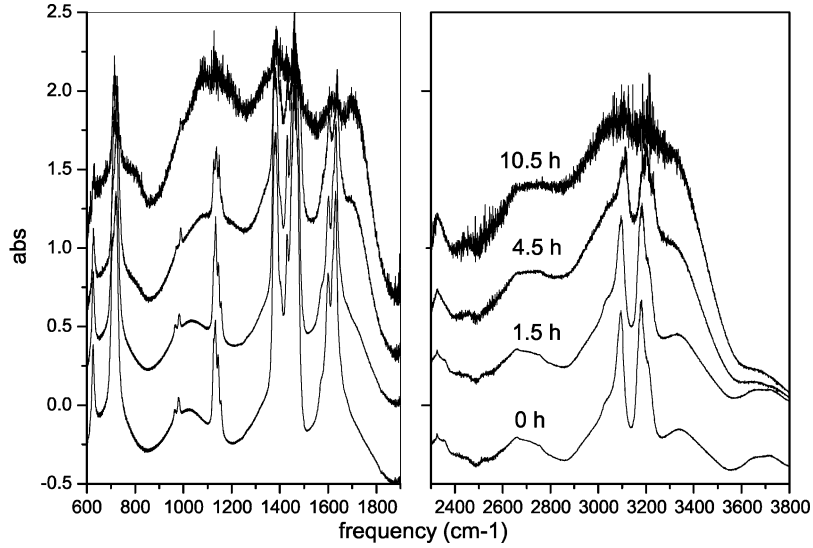

Figure 9. FTIR spectra of a 35 μm thick sample of nitromethane at 18.5 GPa as a function of the irradiation time (irradiation performed with 100 mW at 458 nm).

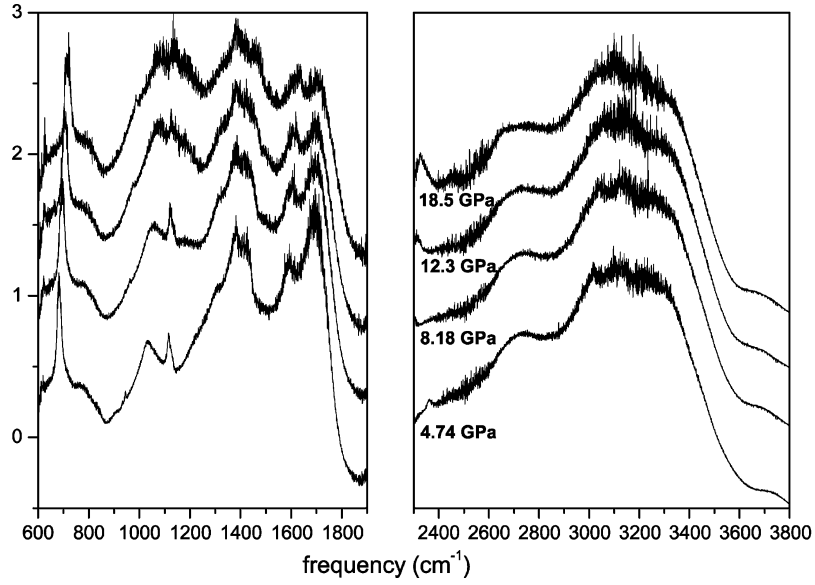

Figure 10. FTIR spectra of nitromethane on decompression after the photoassisted reaction.

is characterized by the intensification of the IR absorptions in the regions 900−1800 and 2600−3500 cm^{-1}. However, some significant differences can be noted. The C═O stretching band at 1700 cm^{-1} assigned to an amidic group is already evident in the spectrum. This can be due to the lower pressure of this experiment. In fact, in the pure pressure experiment, on decreasing the pressure this peak is already clearly seen at 14.6 GPa (see Figure 5). The major difference is the prominence of two peaks at 1370 and at 1030 cm^{-1}. In the high-frequency region of the spectrum, an enhancement of the intensity around 3200 cm^{-1} is observed.

The effect of decreasing the pressure on the infrared spectrum is shown in Figure 10. On complete unloading of the membrane pressure, a residual pressure of 4.74 GPa is still present on the sample, whereas the cell opening caused a complete loss of the sample, as happened in all the experiments where no KBr pellet was used. Also in this case an overall loss of intensity of the broad band centered at 1200 cm^{-1} is observed, while the amidic band at 1700 cm^{-1} increases to finally become the most intense band of the spectrum. At low pressure, the antisymmetric stretching mode of carbon dioxide is observed again. The nitromethane bands at 710 and 1030 cm^{-1} are unchanged on decreasing the pressure: their relative intensity is the same as in the initial spectrum of the experiment, and this confirms their assignment to nitromethane. The peaks at 1370 and 1030 cm^{-1} that represent the most evident difference with respect to the purely pressure-induced reaction do not change substantially upon unloading. In conclusion, apart from the residual bands of nitromethane, the spectrum of the sample after unloading the pressure looks like a superposition of the spectrum of *N*-methylformamide and that of other species that can be most likely identified as methanol, whose most intense band falls around 1030 cm^{-1}, and ammonium carbonate, assuming that the three bands of this compound below 1500 cm^{-1} [41] are broadened and overlapped with the *N*-methylformamide band falling in this same region (see Figure 10). The formation of an ammonium salt is not really surprising. In fact, Brasch[9] already reported on the possible formation of ammonium oxalate in the thermal decomposition of nitromethane. Piermarini et al.[4] reported that the pressure decomposition of nitromethane above 400 K produces ammonium formate even though the limited region of the spectrum does not allow for this identification with

certainty. On the other side, experiments on $H_2O/CO_2/NH_3$ mixtures resulted in the formation of ammonium bicarbonate under shock synthesis[42] or on the formation of ammonium carbamate in thermal processes.[43] On closer observation, it seems that the spectral features assigned to ammonium carbonate are also weakly present in the product of the pure pressure reaction and are washed out on cell opening (Figure 6). The formation of methanol is consistent with the known photochemistry of nitromethane. In fact, photodissociation of gas-phase nitromethane causes primarily the omolythic cleavage of the C−N bond, through excitation of either the $\pi \rightarrow \pi^*$ or the $\sigma \rightarrow \pi^*$ transition.[44] The C−N bond breaking was identified as the main primary process also in the nitromethane photodissociation in the liquid phase[45] and in the Ar matrix at 14 K,[46] as well as in higher nitroalkanes.[47] Our finding of the possible methanol formation at high pressure, occurring only in the photoassisted reaction, strongly suggests that the C−N bond photodissociation also occurs in the bulk crystalline phase of nitromethane.

Conclusions

The high-pressure chemical reaction of nitromethane shows some peculiar features compared to other molecular crystals investigated so far. A number of crystals, including N_2,[48,49] CO_2,[50] and formic acid,[51] polymerize at high pressure and transform in 3-dimensional arrays that cannot be quenched at ambient conditions. In these systems, the reaction is reversible, and at ambient pressure the original molecular system is fully recovered. Small unsaturated hydrocarbons like acetylene,[52] ethylene,[53] and butadiene,[54] on the contrary, polymerize completely at high pressures, and the polymer can be recovered. Depending on the reaction conditions, and in particular on photophysical activation, conformationally[54] or crystalline[53] pure polymers can be recovered. A still different behavior is observed for aromatics like benzene[55] and furan[28] which are unable to react completely at high pressures giving an admixture of an amorphous material and the reactant. On releasing the pressure, the residual reactant further transforms into the amorphous tridimensional polymer. As described, nitromethane fully transforms at high pressure in a tridimensional array which is intrinsically unstable but does not revert to the original reactant. The high-pressure product decomposes on decreasing the pressure in a number of small volatile molecules, only in part identified, that are lost at zero pressure and on cell opening. As a whole, the chemical decomposition of nitromethane under hydrostatic pressure is not dramatically dissimilar from that under shock loading since small volatile molecules are ultimately obtained in both cases. However, under hydrostatic pressure the reaction proceeds smoothly and in two quite distinct stages. Therefore, the idea that studying the nitromethane under static pressure can give information on the reaction mechanism that is useful also under shock loading is fully supported by the experiments.

From kinetic analysis at two different pressures, further evidence has been gathered in favor of a bimolecular reaction mechanism in the first stage of the reaction. This is also evidenced by the ab initio molecular dynamics simulation showing that the reaction is triggered by an intermolecular H^+ transfer to form a CH_3NOOH^+ species and the aci-ion $CH_2NO_2^-$. This reaction step nicely correlates with the high-pressure crystal structure of nitromethane dominated by a tridimensional network of fairly strong hydrogen bonds. This is a nice demonstration of the relevance of the topochemical principle[56] in solid state reactivity, allowing for reactions occurring with minimum atomic displacements. The topochemical principle does not apply further to the reaction stages on pressure unloading when the small molecules forming from the product decomposition likely acquire an increased mobility.

The recovered products, once volatile molecules are eliminated, include *N*-methylformamide and ammonium carbonate. The recovery of *N*-methylformamide, a molecule containing the prototype peptide bond, is a remarkable result since formamide is considered a possible key molecule for the formation of complex biochemical systems.[57] The formation of formamide has been reported from reactions of elementary molecules containing H, C, O, and N atoms that are indeed the atomic constituents of nitromethane. *N*-Methylformamide does not form directly from nitromethane but most likely from the small molecules arising from the decomposition of the high-pressure product. The interesting point is that *N*-methylformamide forms in the absence of any catalytic support exploiting the increased density at high pressure. On the other side, the formation of an ammonium salt has been reported by several authors both from nitromethane decomposition and from catalyzed reactions of simple molecules. The presence of methanol as a product only in the photoassisted reaction is perfectly consistent with the known photochemistry of nitroalkanes that photodissociate through the C−N bond cleavage. This represents a new reaction channel competing in the crystal with the one observed in the purely pressure-induced reaction.

Acknowledgment. This work was supported by the European Union FP7 G.A.No 228334-LASERLAB EUROPE, by the Italian Ministero dell'Università e della Ricerca Scientifica e Tecnologica (MURST), and by "Firenze Hydrolab" through a grant by Ente Cassa di Risparmio di Firenze. We would like to thank the CINECA supercomputer center for a generous allocation of computer time.

Supporting Information Available: Graphic showing some of the molecules isolated at the end of the simulations at 300 K and graphic showing some of the molecules isolated at the end of the simulations at 750 K. This material is available free of charge via the Internet at http://pubs.acs.org.

References and Notes

(1) Manaa, M. R.; Fried, M. E.; Melius, C. F.; Elstner, M.; Frauenheim, Th. *J Phys. Chem. A* **2002**, *106*, 9024–9029.

(2) Crawforth, C. G.; Waddington, D. J. *Trans. Faraday Soc.* **1969**, *65*, 1334–1349.

(3) Wang, J.; Brower, K. R.; Naud, D. L. *J. Org. Chem.* **1997**, *62*, 9048–9054.

(4) Piermarini, G. J.; Block, S.; Miller, P. J. *J. Phys. Chem.* **1989**, *93*, 457–462.

(5) Pangilinan, G. I.; Gupta, Y. M. *J. Phys. Chem.* **1994**, *98*, 4522–4529.

(6) Winey, J. M.; Gupta, Y. M. *J. Phys. Chem. B* **1997**, *101*, 10733–10743.

(7) Bardo, R. D. *Proceedings of the Eighth Symposyum (Int.) on Detonation*, NSWC MP 86−194, NSWC White Oak, Silver Spring, MD 20903-5000, Albuquerque, NM, July 15, 1985.

(8) Manaa, M. R.; Reed, E. J.; Fried, L. E.; Galli, G.; Gygi, F. *J. Chem. Phys.* **2004**, *120*, 10146–10153.

(9) Brasch, J. W. *J. Phys. Chem.* **1980**, *84*, 2084–2085.

(10) Constantinou, C. P.; Winey, J. M.; Gupta, Y. M. *J. Phys. Chem.* **1994**, *98*, 7767–7776.

(11) Engelke, R.; Earl, W. L.; Rohlfing, C. M. *J. Chem. Phys.* **1986**, *84*, 142–146.

(12) Engelke, R.; Schiferl, D.; Storm, C. B.; Earl, W. L. *J. Phys. Chem.* **1988**, *92*, 6815–6819.

(13) Engelke, R.; Earl, W. L.; Rohlfing, C. M. *J. Phys. Chem.* **1986**, *90*, 545–547.

(14) Courtecuisse, S.; Cansell, F.; Fabre, D.; Petitet, J.-P. *J. Chem. Phys.* **1995**, *102*, 968–974.

(15) Pruzan, Ph.; Canny, B.; Power, C.; Chervin, J. C. *Proceedings of the XVII International Conference on Raman Spectoscopy (ICORS 2000)*; Zhang, S.-L., Zhu, B.-f., Ed.; John Wiley and Sons: New York, 2000; p 142.

(16) Citroni, M.; Datchi, F.; Bini, R.; Di Vaira, M.; Pruzan, Ph.; Canny, B.; Schettino, V. *J. Phys. Chem. B* **2008**, *112*, 1095–1103.

(17) Bini, R.; Ballerini, R.; Pratesi, G.; Jodl, H. J. *Rev. Sci. Instrum.* **1997**, *68*, 3154–3160.

(18) Car, R.; Parrinello, M. *Phys. Rev. Lett.* **1985**, *55*, 2471–2474.

(19) Hutter, J.; Alavi, A.; Deutch, T.; Bernasconi, M.; Goedecker, St.; Marx, D.; Tuckerman, M.; Parrinello, M. *CPMD*; MPI für Festkörperforschung and IBM Zurich Research Laboratory: Stuttgart, 1995−1999.

(20) Becke, A. D. *J. Chem. Phys.* **1993**, *98*, 5648–5652.

(21) Lee, C.; Yang, W.; Parr, R. G. *Phys. Rev. B* **1988**, *37*, 785–789.

(22) Troullier, N.; Martins, J. L. *Phys. Rev. B* **1991**, *43*, 1993–2006.

(23) Kleinman, L.; Bylander, D. M. *Phys. Rev. Lett.* **1982**, *48*, 1425–1428.

(24) Conroy, M. W.; Oleynik, I. I.; Zybin, S. V.; White, C. T. *J. Phys. Chem. A* **2009**, *113*, 3610–3614.

(25) Mazari, N.; Vanderbilt, D. *Phys. Rev. B* **1997**, *56*, 12848–12865.

(26) Silvestrelli, P. L.; Mazari, N.; Vanderbilt, D.; Parrinello, M. *Solid State Commun.* **1998**, *107*, 7–11.

(27) Silvestrelli, P. L. *Phys. Rev. B* **1999**, *59*, 9703–9706.

(28) Ceppatelli, M.; Santoro, M.; Bini, R.; Schettino, V. *J. Chem. Phys.* **2003**, *118*, 1499–1506.

(29) Neumann, M. A.; Perrin, M. A. *J. Phys. Chem. B* **2005**, *109*, 15531–15541.

(30) Albrecht, M.; Rice, C. A.; Suhm, M. A. *J. Phys. Chem. A* **2008**, *112*, 7530–7542.

(31) Gaigeot, M. P.; Vuilleumier, R.; Sprik, M.; Borgis, D. *J. Chem. Theory Comput.* **2005**, *1*, 772–789.

(32) Allnat, A. R.; Jacobs, P. W. M. *Can. J. Chem.* **1968**, *46*, 111. Jacobs, P. W. M. *J. Phys. Chem. B* **1997**, *101*, 10086–10093.

(33) Walker, I. C.; Fluendy, M. A. D. *Int. J. Mass Spectrom.* **2001**, *205*, 171–182.

(34) Flicker, W. M.; Mosher, O. A.; Kuppermann, A. *J. Chem. Phys.* **1980**, *72*, 2788–2794.

(35) Reed, E. J.; Jannopulos, J. D.; Fried, L. E. *Phys. Rev. B* **2000**, *62*, 16500–16509.

(36) Liu, H.; Zhao, J.; Wei, D.; Gong, Z. *J. Chem. Phys.* **2006**, *124*, 124501–124510.

(37) Margetis, D.; Kaxiras, E.; Elstner, M.; Frauenheim, Th.; Manaa, M. R. *J. Chem. Phys.* **2002**, *117*, 788–799.

(38) Bini, R. *Acc. Chem. Res.* **2004**, *37*, 95–101.

(39) Citroni, M.; Bini, R.; Foggi, P.; Schettino, V. *Proc. Natl. Acad. Sci.* **2008**, *105*, 7658–7663.

(40) Citroni, M.; Costantini, B.; Bini, R.; Schettino, V. *J. Phys. Chem. B* **2009**, *113*, 13526–13535.

(41) Peeters, Z.; Hudson, R. L.; Moore, M. H.; Lewis, A. *The formation and stability of carbonic acid on outer solar system bodies*; 2009; http://ntrs.nasa.gov, document ID: 20090033103.

(42) Price, M. C.; Burchell, M. J.; Miljkovic, K.; Kearsley, A. T.; Cole, M. J. *Shock synthesis of organics from simple ice mixtures*, 41 Lunar and Planetary Science Conference, The Woodlands, TX, March 1−5, 2010.

(43) Bossa, J. B.; Theulé, P.; Duvernay, M.; Borget, F.; Chiavassa, T. *Astron. Astrophys.* **2008**, *492*, 719–724.

(44) Wade, E. A.; Reak, K. E.; Li, S. L. *J. Phys. Chem. A* **2006**, *110*, 4405–4412, and references therein.

(45) Jarosiewicz, M.; Szychlinski, J.; Piszczek, L. *J. Photochem.* **1985**, *29*, 343–351.

(46) Jacox, M. E. *J. Phys. Chem.* **1984**, *88*, 3373–3379.

(47) Ross, P. L.; Van Bramen, S. E.; Johnston, M. V. *Appl. Spectrosc.* **1996**, *50*, 608–613.

(48) Eremets, M. I.; Hemley, R. J.; Mao, H. K.; Gregoryanz, E. A. *Nature* **2001**, *411*, 170–174.

(49) Eremets, M. I.; Gavriliuk, A. G.; Trojan, I. A.; Dzivenko, D. A.; Boehler, R. *Nat. Mater.* **2004**, *3*, 558–563.

(50) Santoro, M.; Gorelli, F. A.; Bini, R.; Ruocco, G.; Scandolo, S.; Crichton, W. *Nature* **2006**, *441*, 857–860.

(51) Goncharov, A. F.; Manaa, M. R.; Zaug, J. M.; Gee, R. H.; Fried, L. E.; Montgomery, W. B. *Phys. Rev. Lett.* **2005**, *94*, 065505.

(52) Ceppatelli, M.; Santoro, M.; Bini, R.; Schettino, V. *J. Chem. Phys.* **2000**, *113*, 5991–6000.

(53) Chelazzi, D.; Ceppatelli, M.; Santoro, M.; Bini, R.; Schettino, V. *J. Phys. Chem. B* **2005**, *109*, 21658–21663.

(54) Citroni, M.; Ceppatelli, M.; Bini, R.; Schettino, V. *J. Chem. Phys.* **2003**, *118*, 1815–1820.

(55) Ciabini, L.; Santoro, M.; Bini, R.; Schettino, V. *J. Chem. Phys.* **2002**, *116*, 2928–2935.

(56) Cohen, M. D.; Schmidt, G. M. J. *J. Chem. Soc.* **1964**, 1996–2000.

(57) Saladino, R.; Crestini, C.; Ciciriello, F.; Costanzo, G.; Di Mauro, E. *Chem. Biodiversity* **2007**, *4*, 694–720.

JP1035508